



Salen complex of Cu(II) supported on superparamagnetic Fe₃O₄@SiO₂ nanoparticles: an efficient and magnetically recoverable catalyst for N-arylation of imidazole with aryl halides

Ali Reza Sardarian¹ · Neda Zohourian-Mashmoul¹ · Mohsen Esmailpour¹

Received: 1 December 2017 / Accepted: 8 January 2018
© Springer-Verlag GmbH Austria, part of Springer Nature 2018

Abstract

The Fe₃O₄@SiO₂/Salen-Cu(II) nanocatalyst is reported as a thermally and air-stable, economical, and magnetically recoverable heterogeneous catalyst for the selective and efficient N-(hetero)arylation of imidazole. Only by adding a small amount of the catalyst (0.4 mol% Cu) to the reactants and heating under air, the new presented method provides a variety of functionalized and hindered N-(hetero)arylimidazoles in good to excellent yields within short reaction times. The catalyst could be easily recovered with the aid of a permanent magnet and reused up to five consecutive runs without significant loss of activity. Also, the leaching of Cu was negligible after the fifth recycle. Particularly, using either (hetero)aryl iodides or bromides as arylating agents and the need of only small amount of the magnetically recoverable heterogeneous copper-based nanocatalyst make this method low-cost, environmentally benign, and easy to use.

Graphical abstract



Keywords N-Arylation · Aryl halides · Heterogeneous catalysis · Magnetic properties · Nanostructures · Salen-Cu(II)

Electronic supplementary material The online version of this article (<https://doi.org/10.1007/s00706-018-2148-4>) contains supplementary material, which is available to authorized users.

✉ Ali Reza Sardarian
sardarian@shirazu.ac.ir

¹ Chemistry Department, College of Sciences, Shiraz University, Shiraz 71946 84795, Iran

Introduction

Taking a look at the literature, we will find out that *N*-heterocyclic compounds are prevalent structural motifs in biological, pharmaceutical, chemical, and material fields [1–3]. Among these, imidazole derivatives are utilized not only in medicinal field as cardiotoxic, antiglaucoma, antibacterial, antimycotic, antiviral, and antitumor agents [4–8], but also in drug development since they can form soluble salts, which make the drugs bioavailable and orally absorbable [9]. Furthermore, these derivatives have been widely applied in the area of organic chemistry as important building blocks for the synthesis of *N*-heterocyclic

carbenes [10], a privileged class of ligands for transition-metal catalysis [11], and for the synthesis of room temperature ionic liquids, which are environmentally benign solvents for organic synthesis [12].

Generally, *N*-arylimidazole compounds can be synthesized via nucleophilic aromatic substitution of imidazoles with aryl halides [13], which is limited to those aryl halides bearing electron-withdrawing substituents or via transition-metal catalyzed *N*-arylation of imidazoles [14], which has been proven to be the most efficient and useful method for the synthesis of *N*-arylimidazole derivatives. The tendency to create inexpensive and environmentally friendly catalytic systems led to develop copper-catalyzed *N*-arylation of imidazoles with aryl halides, which was pioneered by Buchwald [15]. Arylboronic acids [16], aryllead triacetates [17], hypervalent iodonium salts [18], and triarylbismuths [19] are the other types of reagents that have been employed instead of aryl halides for Cu-mediated *N*-arylation of imidazoles. However, the major drawbacks of employing these kinds of aryl donors are the use of toxic, less available, high cost, and/or unstable reagents that can be difficult to access. For increasing the yields of the products as well as decreasing time, temperature, toxicity, and the cost of the imidazole *N*-arylation reaction, various copper catalysts have been developed to date [20, 21]. Most of the utilized catalysts are homogeneous and, despite their high activity, the difficulties associated with the separation and recovery of them limit their use, especially in pharmaceutical industry in which the final products must be free of metal contamination [22–24]. Although heterogenization of the catalysts, by grafting them on a solid support surface or trapping them inside the pores of the support, makes them separable, reusable, and benign, it is accepted that heterogeneous catalysts are less active than homogeneous ones due to their less accessible active sites [25]. With the development of the nanotechnology, creating nanosized heterogeneous catalysts, which possess the recoverability of heterogeneous catalysts, together with the high activity of the homogeneous ones (due to their large surface-to-volume ratio), has become an attractive alternative [26–29]. However, the separation and recovery of such catalysts by using conventional techniques (such as centrifugation or filtration) are cumbersome because of their nanometric size [30, 31]. To overcome this issue, the nanocatalysts must be supported on insoluble magnetically separable surfaces such as core–shell structures in which, generally, iron oxides as magnetic cores have been coated with organic or inorganic layers to prevent aggregation phenomenon [32]. Of different iron oxides, Fe_3O_4 is the most magnetic mineral in the nature and its biocompatibility has been proved [33, 34]. Also, of different iron oxides coating materials, silica coating is widely reported since the silica surfaces bestow not only facile

functionalization, but also chemical and thermal stability to these magnetic cores [34–39]. Therefore, among the various magnetic core–shell structures, $\text{Fe}_3\text{O}_4@ \text{SiO}_2$ is a very promising candidate.

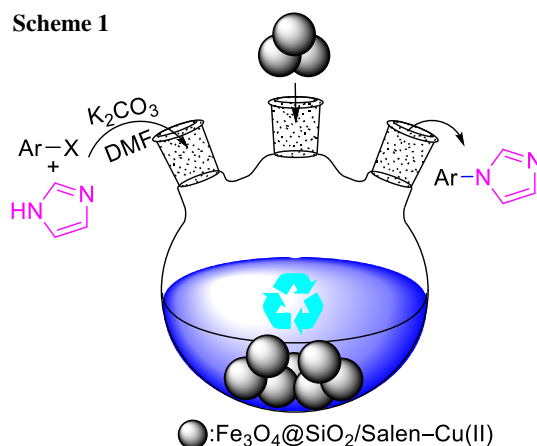
Recently, a few examples of utilizing copper-based magnetic nanocatalysts for imidazole *N*-arylation have been reported, which, unfortunately, suffer from the need of prolonged reaction times, excess base, high copper loading, limited substrate scope, and/or protecting by an inert gas [40–42].

Considering widespread applications of *N*-arylimidazole derivatives and encouraged by the remarkable performance of magnetic copper nanocatalysts [40–42], and Salen-Cu(II) complexes (as inexpensive and air-/moisture-stable catalysts) [43] in the *N*-arylation of imidazoles, we became interested in developing a new, simple, and efficient synthetic protocol for the *N*-arylation of imidazole using salen complex of Cu(II) supported on superparamagnetic $\text{Fe}_3\text{O}_4@ \text{SiO}_2$ nanoparticles as illustrated in Scheme 1 to overcome above-mentioned drawbacks.

Results and discussion

The preparation steps of the $\text{Fe}_3\text{O}_4@ \text{SiO}_2/\text{Salen-Cu(II)}$ nanocatalyst, as described in experimental section, have been depicted in Fig. 1, briefly. Firstly, Fe_3O_4 nanocore was prepared using Fe(II) and Fe(III) chloride salts, and then coated by silica shell using TEOS as the silica source to give $\text{Fe}_3\text{O}_4@ \text{SiO}_2$ core–shell structure [44].

The Fe_3O_4 , $\text{Fe}_3\text{O}_4@ \text{SiO}_2$, and $\text{Fe}_3\text{O}_4@ \text{SiO}_2/\text{Salen-Cu(II)}$ nanocatalyst were characterized by FT-IR, XRD, FE-SEM, DLS, and ICP methods [44]. As can be seen in Fig. 1, FE-SEM image of the catalyst shows the morphology of the catalyst, and reveals the spherical-shaped



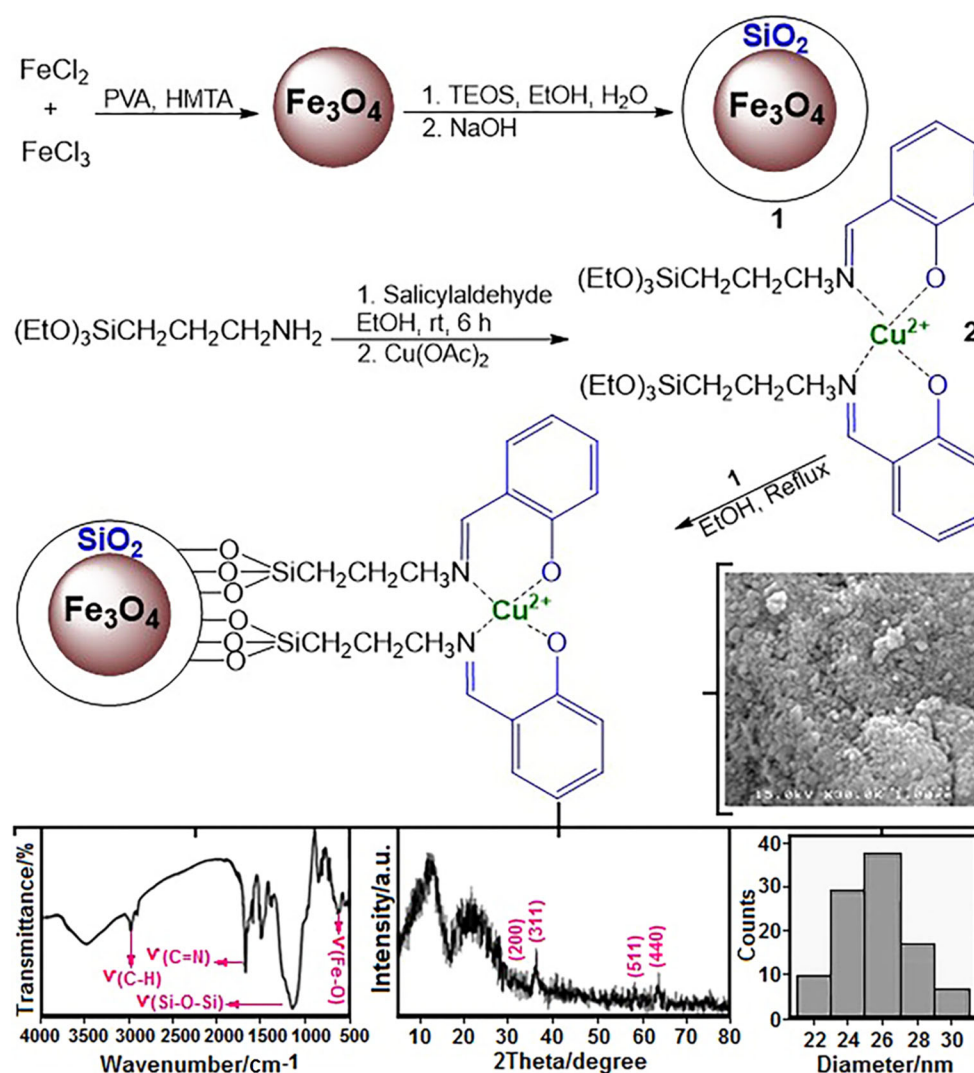


Fig. 1 The Fe₃O₄@SiO₂/Salen-Cu(II) nanocatalyst preparation sequence and its characterization by FE-SEM, FT-IR, XRD, and DLS techniques

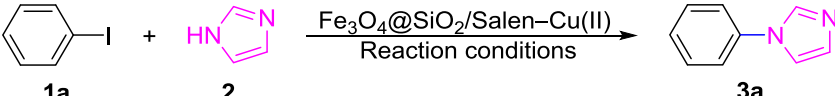
Fe₃O₄@SiO₂/Salen-Cu(II) nanoparticles. The analysis of the FT-IR spectrum of the catalyst (Fig. 1), based on the presence of distinctive vibrational bands in 3400 (O–H stretching), 2750–3000 (C–H stretching), 1622 (C=N stretching), 1000–1150 (Si–O–Si asymmetric stretching), and 571 (Fe–O stretching) cm⁻¹, demonstrates the formation of Fe₃O₄@SiO₂/Salen-Cu(II) nanocatalyst.

As shown in powder X-ray diffraction (XRD) pattern (Fig. 1) of the catalyst, the crystalline structure of Fe₃O₄ cores has not been damaged during silica coating and surface functionalization. Using DLS, the size distribution of Fe₃O₄@SiO₂/Salen-Cu(II) nanoparticles is centered around 26 nm (Fig. 1). In addition, as determined by inductively coupled plasma (ICP), the copper loading in this nanocatalyst is 0.21 mmol/g [44].

After the preparation and characterization of the Fe₃O₄@SiO₂/Salen-Cu(II) nanocatalyst, its catalytic

activity in the N-arylation of imidazole with aryl halides was evaluated. Initially, to identify the optimized reaction conditions, iodobenzene (**1a**) and imidazole (**2**) were selected as model substrates. In the following, the effect of different amounts of the catalyst, various solvents, bases, temperatures (Table 1) and Fe₃O₄@SiO₂/Salen complex of different metal ions were investigated on the reaction (Table 2).

We started to optimize the reaction temperature of imidazole N-arylation with iodobenzene in the presence of the Fe₃O₄@SiO₂/Salen-Cu(II) complex as catalyst, DMF as solvent and K₂CO₃ as base. As can be seen from Table 1, temperature plays a significant role in this reaction. By raising the temperature to 120 °C, the reaction time decreases to 1.5 h and the yield of the desired product increases substantially (Table 1, entry 4). Then, we evaluated the optimal amount of the catalyst, which is found to be as low as 0.02 g

Table 1 Optimization of the reaction conditions for the Fe₃O₄@SiO₂/Salen–Cu(II) catalyzed N-arylation of imidazole with iodobenzene


Entry	Solvent	Base	Catalyst/mol% Cu	Temp/°C	Time/h	Yield ^a /%
1	DMF	K ₂ CO ₃	0.6	R.T.	24	0
2	DMF	K ₂ CO ₃	0.6	70	24	Trace
3	DMF	K ₂ CO ₃	0.6	100	24	15
4	DMF	K ₂ CO ₃	0.6	120	1.5	81
5	DMF	K ₂ CO ₃	0.6	Reflux	1.5	79
6	DMF	K ₂ CO ₃	–	Reflux	4	0
7	DMF	K ₂ CO ₃	0.2	120	4	70
8	DMF	K ₂ CO ₃	0.4	120	1.5	81
9	DMF	K ₂ CO ₃	0.8	120	1.5	78
10	DMSO	K ₂ CO ₃	0.4	Reflux	1.5	76
11	CH ₃ CN	K ₂ CO ₃	0.4	Reflux	24	47
12	1,4-Dioxane	K ₂ CO ₃	0.4	Reflux	24	14
13	Toluene	K ₂ CO ₃	0.4	Reflux	24	12
14	Solvent-free	K ₂ CO ₃	0.4	100	24	10
15	Solvent-free	K ₂ CO ₃	0.4	150	4	45
16	H ₂ O	K ₂ CO ₃	0.4	Reflux	24	0
17	MeOH	K ₂ CO ₃	0.4	Reflux	24	0
18	DMF	–	0.4	120	24	20
19	DMF	<i>t</i> -BuONa	0.4	120	1.5	78
20	DMF	Cs ₂ CO ₃	0.4	120	1.5	80
21	DMF	Et ₃ N	0.4	120	24	22
22	DMF	K ₃ PO ₄	0.4	120	2	76
23	DMF	NaOH	0.4	120	1.5	80
24	DMF	K ₂ CO ₃ ^b	0.4	120	1.5	82
25	DMF	K ₂ CO ₃	0.4	120	4	15 ^c

Reaction conditions: iodobenzene (1.0 mmol), imidazole (2.0 mmol), base (2.0 mmol), Fe₃O₄@SiO₂/Salen–Cu(II) catalyst, in 2.5 cm³ solvent and under air atmosphere, unless otherwise stated

^aIsolated yield

^bThe reaction was performed using 1.0 mmol of base

^cThe reaction was performed using 1.0 mmol of imidazole

(0.4 mol%), and no obvious improvement is observed using greater amounts of the catalyst (Table 1, entries 4, 8, and 9). Of the different solvents tested, DMF is demonstrated to be the most effective one for this reaction (Table 1, entry 8). It is notable that aprotic polar solvents, such as DMF and DMSO, are much more effective than those with lower dipolar moment or solvent-free conditions, while protic polar ones, such as H₂O and MeOH, are ineffective (Table 1, entries 8, 10–17). Further investigation indicated that in the absence of any added base, only 20% yield is obtained within 24 h (Table 1, entry 18). Subsequently, in base optimization, the use of *t*-BuONa, Cs₂CO₃, K₂CO₃, and NaOH

result in higher yields among those listed in Table 1 (entries 8, 19–23). Consequently, K₂CO₃ was chosen as the most favorable base, since it is a stable, cheap, and weak base. Particularly noteworthy is that the coupling product **3a** is obtained almost in the same yield when either stoichiometric or excess amount of K₂CO₃ was used (Table 1, entries 8 and 24). It is observed that the addition of 1 mmol of imidazole, instead of 2 mmol, causes a decrease in the yield of product to 15% (Table 1, entry 25).

Finally, the optimization was completed by comparing the activity of Fe₃O₄@SiO₂/Salen complex of Cu²⁺ with Fe₃O₄ and Fe₃O₄@SiO₂/Salen complex of some other metal ions

Table 2 Comparison of the activity of Fe₃O₄@SiO₂/Salen complex of different metal ions in the N-arylation of imidazole with iodobenzene

Entry	Metal ion	Time/h	Yield ^a /%
1	Co ²⁺	24	0
2	Cr ³⁺	24	0
3	Cu ²⁺	1.5	82
4	Fe ²⁺	24	0
5	Mn ²⁺	24	0
6	Zn ²⁺	24	0
7	Fe ₃ O ₄ ^b	24	0

Reaction conditions: iodobenzene (1.0 mmol), imidazole (2.0 mmol), K₂CO₃ (1.0 mmol), corresponding metal ion catalyst (0.02 g, 0.4 mol% Cu), in 2.5 cm³ DMF at 120 °C and under air atmosphere

^aIsolated yield

^bThe reaction was proceeded using Fe₃O₄ as catalyst

such as Co²⁺, Cr³⁺, Fe²⁺, Mn²⁺, Zn²⁺. The results indicated that Fe₃O₄@SiO₂/Salen complex of Cu²⁺ is the only efficient nanocatalyst for such a reaction (Table 2, entry 3).

With the optimized reaction conditions in hand, we further probed the scope of this methodology by employing various derivatives of aryl or heteroaryl halides as imidazole arylating agents (Table 3). From Table 3, it is clear that both the reaction time and yield are dependent to the type of arylating agent, the electronic nature and positions of the substituents, which affect their electronic effects, and also steric hindrance on the corresponding aryl donor. The reactivity of the aryl halides in this reaction follows the trend of iodobenzene > bromobenzene ≫ chlorobenzene, in which iodobenzene and bromobenzene carry out the N-arylation reaction with high yields within 1.5 and 2 h, respectively, whereas chlorobenzene is unreactive toward this reaction even after prolonged heating (Table 3, entries 1–3).

The selectivity of the reaction has been demonstrated using dihalobenzenes (Table 3, entries 4–6). Further experiments indicated that the catalytic system has tolerated both electron-donating and withdrawing substituent groups on the bromo- or iodobenzene (Table 3, entries 4–18). However, considering shorter reaction times and higher yields obtained for electron-deficient *p*- and *m*-substituted aryl iodides and bromides, these aryl halides are found to be more reactive than electron-rich ones (Table 3, entries 4, 6–12, 15–18). The reaction sensitivity to steric hindrance was explored by opting *o*-substituted arylating agents as coupling partners. In this regard, the N-arylation reaction of bromo- or iodobenzenes with both electron donating and withdrawing groups in *ortho* position proceed in longer times along with lower yields (Table 3, entries 5, 13, 14, 19). Moreover, we succeeded to couple

imidazole with both heteroaryl bromide and iodide with excellent yields (Table 3, entries 20 and 21).

In an attempt to couple iodobenzene with benzamide, no arylated product was obtained even after 24 h. Indeed, this result indicated selective arylation of imidazole in the presence of an amide group.

With respect to literature [51], the reactivity order Ar–I > Ar–Br ≫ Ar–Cl and better reactivity of electron-deficient aryl halides than electron-rich ones (Table 3), the plausible mechanism for this catalytic reaction has been depicted in Scheme 2. In the first step, oxidative addition, Cu inserts into the Ar–X bond to form complex II. Subsequently, this complex reacts with base-activated imidazole and, in the following step, undergoes a reductive elimination.

Table 4 provides a comparison of the results obtained for our catalytic system with those have been already reported in literature in the N-arylation reaction of imidazole with 1-bromo-4-chlorobenzene. Requiring to lower copper loading, and easy magnetically recoverability of our heterogeneous catalyst along with higher yield of corresponding products and much shorter reaction time, clearly demonstrate the superiority of the Fe₃O₄@SiO₂/Salen-Cu(II) catalyst among others.

For testing the reusability of the catalyst, iodobenzene was selected to react with imidazole under the optimized conditions. After completion of the reaction, the catalyst was retrieved from the reaction medium by means of an external magnet, washed with solvent, dried, and reused for five consecutive runs without significant loss of activity (Fig. 2a). Checking ICP results of the catalyst revealed that the leaching of copper was negligible.

Figure 2b shows dispersibility of the Fe₃O₄@SiO₂/Salen-Cu(II) nanocatalyst in a solution in the absence of magnetic field, and the catalyst separability with the aid of a permanent magnet. According to FE-SEM image (Fig. 2c), after five repeated reaction cycles, the morphology of the catalyst remained almost unaltered, except that the aggregation of the Cu nanoparticles might have occurred through the leaching/re-deposition phenomenon during the catalytic function. Also, by DLS analyses, the average size of the catalyst nanoparticles was found to be 33 nm after five reaction cycles (Fig. 2d).

Conclusion

In summary, we have offered a new and efficient nanocatalytic system for selective N-arylation of imidazole with aryl iodides and bromides using a magnetically recoverable and reusable heterogeneous Fe₃O₄@SiO₂/

Table 3 N-Arylation of imidazole with aryl halides using Fe₃O₄@SiO₂/Salen-Cu(II) nanocatalyst

Ar-X + $\xrightarrow[\text{K}_2\text{CO}_3, \text{DMF}, 120\text{ }^\circ\text{C}]{\text{Fe}_3\text{O}_4@\text{SiO}_2/\text{Salen-Cu(II)}}$ Ar-N \langle

X = Cl, Br, I

1 **2** **3a-3p**

Entry	X	Ar	Product	Time/h	Yield ^a /%	TON ^b	TOF ^c /h ⁻¹	M.p./°C [References]
1	I	C ₆ H ₅ -	3a	1.5	82	205	136.7	Oil [45]
2	Br	C ₆ H ₅ -	3a	2	75	187.5	93.7	Oil [45]
3	Cl	C ₆ H ₅ -	3a	24	0	0	0	Oil [45]
4	I	4-Br-C ₆ H ₄ -	3b	1	82	205	205	119–120 (120–121 [45])
5	I	2-Br-C ₆ H ₄ -	3c	6	72	180	30	33–34 (33 [46])
6	Br	4-Cl-C ₆ H ₄ -	3d	2	97	242.5	121.2	84–86 (84–86 [47])
7	I	4-(CH ₃ CO)-C ₆ H ₄ -	3e	0.5	86	215	430	111–113 (112–114 [48])
8	I	4-NO ₂ -C ₆ H ₄ -	3f	0.5	85	212.5	425	203–205 (203–205 [47])
9	Br	4-NO ₂ -C ₆ H ₄ -	3f	0.5	84	210	420	203–205 (203–205 [47])
10	Br	3-NO ₂ -C ₆ H ₄ -	3 g	1	83	207.5	207.5	109–110 (109–110 [48])
11	Br	4-CN-C ₆ H ₄ -	3 h	0.5	84	210	420	151–153 (152–154 [49])
12	I	4-CH ₃ -C ₆ H ₄ -	3i	1.5	79	197.5	131.7	Oil [50]
13	I	2-CH ₃ -C ₆ H ₄ -	3j	7	78	195	27.9	Oil [50]
14	Br	2-CH ₃ -C ₆ H ₄ -	3j	48	35	87.5	1.8	Oil [50]
15	Br	3-CH ₃ -C ₆ H ₄ -	3k	3.5	75	187.5	53.6	Oil [47]
16	Br	4-CH ₃ -C ₆ H ₄ -	3i	3.5	74	185	52.9	Oil [50]
17	I		3l	1.5	99	247.5	165	77–79
18	Br	4-CH ₃ O-C ₆ H ₄ -	3m	4.5	71	177.5	39.4	Oil [22]
19	I	1-Naphthyl	3n	24	78	195	8.1	61–63 (63–64 [48])
20	I	3-Thienyl	3o	1.5	97	242.5	161.6	82–84 (82–83 [47])
21	Br	5-Pyrimidinyl	3p	1.5	87	217.5	145	125–127

Reaction conditions: aryl halide (1.0 mmol), imidazole (2.0 mmol), K₂CO₃ (1.0 mmol), Fe₃O₄@SiO₂/Salen-Cu(II) nanocatalyst (0.4 mol%), in DMF (2.5 cm³) at 120 °C and under air atmosphere

^aIsolated yield

^bTON = The number of mmoles of product formed per mmol of catalyst used

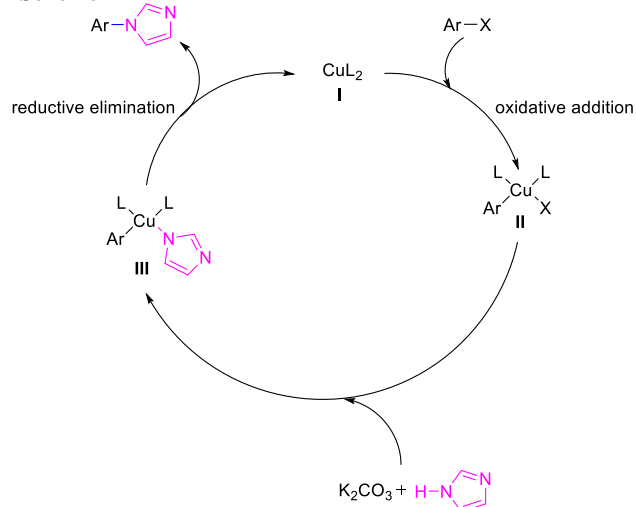
^cTOF = TON per hour

Salen-Cu(II) nanocatalyst. The reusability of the catalyst for several runs with almost consistent activity, as well as requiring only small amount of this catalyst (0.02 g, 0.4 mol% of Cu) for proceeding the reaction successfully, makes our method economical and environmentally benign. This catalytic system not only offers a facile process without the protection of an inert gas, but also is capable of selective coupling of imidazole with wide array of (hetero)aryl iodides and even bromides bearing diverse electronic groups and steric hindrance with good to excellent yields within short reaction times. Moreover, we have employed aryl iodides and bromides as aryl donors, which are less toxic, more cost-effective, and available than other aryl donors have already reported, and stoichiometric amount of base instead of excess amount reported in most examples in literature.

Experimental

All chemical materials were purchased from commercial sources (Merck, Fluka, Aldrich and Acros). Solvents were distilled, dried over the appropriate drying agents, and purified by usual standard methods. Nuclear magnetic resonance (NMR) spectral data were recorded on a Bruker Avance DPX 250 MHz spectrometer using deuterated chloroform (CDCl₃) as solvent and tetramethylsilane (TMS) as an internal reference. Fourier transform infrared spectroscopy (FT-IR) spectra were obtained by a Shimadzu FT-IR 8300 spectrophotometer. Mass spectra were recorded on a Shimadzu GC MS-QP 1000 EX instrument. Field emission scanning electron microscopy (FE-SEM) images were obtained using HITACHI S-4160. Particle sizes of MNPs (magnetic nanoparticles) were

Scheme 2



measured using a HORIBA-LB550 dynamic light scattering (DLS) system. Elemental analyses (C, H, N) were performed using a Thermofinigan Flash EA-1112 CHNSO rapid elemental analyzer. Melting points were determined by Buchi Melting Point B-545 electrical melting point apparatus. Copper loading and leaching tests were carried out by ICP analyzer (Varian, Vista-pro). Progress of the reactions was followed by TLC using silica gel polygrams SIL G/UV 254 plates. Products were purified by column chromatography on Merck Kiesel gel (70–230 mesh), and identified by their melting points, ¹H NMR, ¹³C NMR, FT-IR, and MS spectra subsequently.

General procedure for the preparation of the Fe₃O₄@SiO₂/Salen-Cu(II) nanocatalyst

The Fe₃O₄@SiO₂/Salen-Cu(II) nanocatalyst preparation sequence was reported previously by our research group [44]. Concisely, for preparing Salen-Cu(II) complex,

0.182 g Cu(OAc)₂ (1.0 mmol) was added to the yellow solution of 0.651 g salen ligand (2.0 mmol) in 25 cm³ ethanol, which was obtained from the reaction of 0.176 g 3-aminopropyl(triethoxy)silane (1.0 mmol) and 0.122 g salicylaldehyde (1.0 mmol) in ethanol, and the mixture was stirred at the reflux temperature until we observed completion of the reaction by TLC. Subsequently, 2.0 g Fe₃O₄@SiO₂ magnetic support, which was provided by a modified Stöber method [55, 56], was added to the flask containing Salen-Cu(II) complex (1.0 mmol) in 10 cm³ ethanol, and the mixture was refluxed for 12 h. Ultimately, the Fe₃O₄@SiO₂/Salen-Cu(II) catalyst was magnetically separated, washed with ethanol and deionized water (three times), and then dried at 80 °C.

General procedure for the catalytic N-arylation of imidazole

The reaction flask, containing 0.02 g Cu(II) nanocatalyst (contains 0.4 mol% of Cu(II)), imidazole (2.0 mmol), K₂CO₃ (1.0 mmol), and corresponding aryl halide (1.0 mmol) in 2.5 cm³ DMF, was immersed in a preheated oil bath and the reaction mixture was stirred under air atmosphere at 120 °C until no further conversion of the starting aryl halide was observed by thin-layer chromatography (TLC). After completion of the reaction, the resulting mixture was allowed to cool to room temperature, and then the catalyst was separated out by an external permanent magnet, washed with ethyl acetate (EtOAc) and dried. The residue mixture was diluted by H₂O and extracted with EtOAc (3 × 10 cm³). The extracted organic phases were dried over anhydrous Na₂SO₄, filtrated, concentrated and, finally, purified by silica gel chromatography using petroleum ether/ethyl acetate to afford the corresponding pure N-arylimidazole.

1-(Benzo[d][1,3]dioxol-5-yl)-1H-imidazole (3 I, C₁₀H₈N₂O₂) Pale brown solid; m.p.: 77–79 °C; ¹H NMR

Table 4 Comparison of the activity of different copper catalysts in the N-arylation reaction of imidazole with 1-bromo-4-chlorobenzene

Entry	Catalyst/mol% Cu	Conditions	Time/h	Yield/% ^a	References
1	CuI (30)	[Bmim]BF ₄ , K ₂ CO ₃ , 0 °C	24	80	[47]
2	Cu ₂ O (10)	DMF, <i>t</i> -BuOK, 130 °C	24	95	[52]
3	CuI (10)	DMSO, K ₂ CO ₃ , 125 °C	24	89	[53]
4	Cu ₂ O/ZnO (7.4)	DMSO, KOH, 100 °C	6	80	[54]
5	CuNPs/MagSilica (11)	DMF, K ₂ CO ₃ , 152 °C	32	45 ^b	[41]
6	Salen-Cu(II) complex (10)	DMSO, NaOH, 100 °C	12	49 ^c	[43]
7	Fe ₃ O ₄ @SiO ₂ /Salen-Cu(II) complex (0.4)	DMF, K ₂ CO ₃ , 120 °C	2	97	This study

^aIsolated yield

^bTogether with 10% of the corresponding bis-imidazole product

^cAryl halide used in this work is 1-bromo-4-nitrobenzene

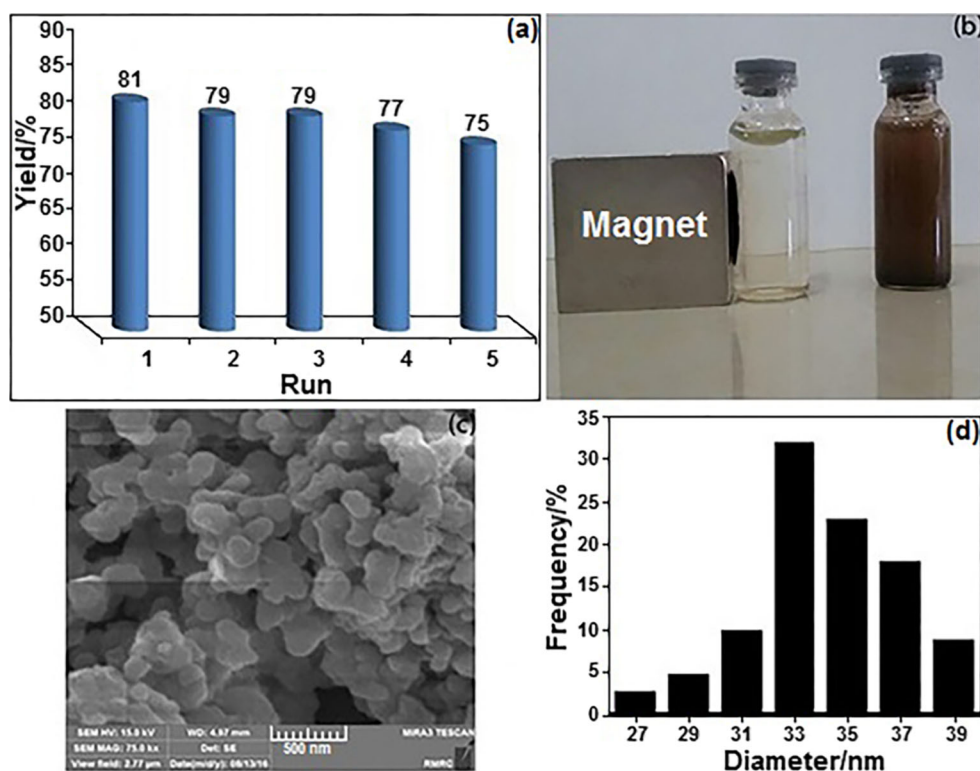


Fig. 2 **a** Recyclability of $\text{Fe}_3\text{O}_4@/\text{SiO}_2/\text{Salen-Cu(II)}$ nanocatalyst in the synthesis of **3a**; **b** photograph of dispersed, and magnetically attracted $\text{Fe}_3\text{O}_4@/\text{SiO}_2/\text{Salen-Cu(II)}$ nanocatalyst in a solution,

separately; **c** FE-SEM and **d** DLS images of $\text{Fe}_3\text{O}_4@/\text{SiO}_2/\text{Salen-Cu(II)}$ nanoparticles after five repeated reaction cycles

(250 MHz, CDCl_3): $\delta = 7.61$ (s, 1H), 7.04–7.02 (m, 2H), 6.73–6.65 (m, 3H), 5.87 (s, 2H) ppm; ^{13}C NMR (62.9 MHz, CDCl_3): $\delta = 148.4$, 146.8, 135.73, 131.6, 129.9, 118.7, 114.9, 108.5, 103.4, 101.9 ppm; IR (KBr): $\bar{\nu} = 3121$, 3097, 3070, 2989, 2912, 1840, 1689, 1612, 1508, 1454, 1381, 1311, 1230, 1111, 1049, 1034, 980, 926, 872, 810, 744, 660, 617, 579, 482, 436 cm^{-1} ; MS (70 eV): m/z (%) = 189 (M^++1 , 3.7), 188 (M^+ , 18.2).

5-(1H-Imidazol-1-yl)pyrimidine (3p, $\text{C}_7\text{H}_6\text{N}_4$) White solid; m.p.: 125–127 °C; ^1H NMR (250 MHz, CDCl_3): $\delta = 9.16$ (s, 1H), 8.83 (s, 2H), 7.87 (s, 1H), 7.29 (s, 1H), 7.24 (s, 1H) ppm; ^{13}C NMR (62.9 MHz, CDCl_3): $\delta = 157.4$, 149.4, 135.2, 132.4, 131.8, 117.6 ppm; IR (KBr): $\bar{\nu} = 3109$, 3040, 3005, 2932, 1682, 1578, 1500, 1454, 1427, 1311, 1262, 1188, 1099, 1065, 957, 906, 744, 717, 652, 629, 613 cm^{-1} ; MS (70 eV): m/z (%) = 148 (M^++2 , 2.4), 147 (M^++1 , 7.9).

Acknowledgements We would like to gratefully acknowledge financial support of this work by research council of Shiraz University.

References

- Grauer A, Späth A, Ma D, König B (2009) Chem Asian J 4:1134
- Güngör T, Fouquet A, Teulon JM, Provost D, Cazes M, Cloarec A (1992) J Med Chem 35:4455
- Herrmann WA (2002) Angew Chem Int Ed 41:1290
- Sircar I, Duell BL, Bobowski G, Bristol JA, Evans DB (1985) J Med Chem 28:1405
- Lo YS, Nolan JC, Maren TH, Welstead WJ Jr, Gripshover DF, Shamblee DA (1992) J Med Chem 35:4790
- Rani N, Sharma A, Singh R (2013) Mini Rev Med Chem 13:1812
- Heeres J, Backx LJJ, Mostmans JH, Cutsem JV (1979) J Med Chem 22:1003
- Al-Masoudi NA, Al-Soud YA, Kalogerakis A, Pannecouque C, De Clercq E (2006) Chem Biodivers 3:515
- Leeson PD, Springthorpe B (2007) Nat Rev Drug Discov 6:881
- Nyce GW, Glauser T, Connor EF, Möck A, Waymouth RM, Hedrick JL (2003) J Am Chem Soc 125:3046
- Harkal S, Rataboul F, Zapf A, Fuhrmann C, Riermeier T, Monsees A, Beller M (2004) Adv Synth Catal 346:1742
- Suárez-Pantiga S, Rubio E, Alvarez-Rúa C, González JM (2009) Org Lett 11:13
- Venuti MC, Stephenson RA, Alvarez R, Bruno JJ, Strosberg AM (1988) J Med Chem 31:2136
- Priyarega S, Raja DS, Babu SG, Karvembu R, Hashimoto T, Endo A, Natarajan K (2012) Polyhedron 34:143
- Kiyomori A, Marcoux JF, Buchwald SL (1999) Tetrahedron Lett 40:2657
- Wu CD, Li L, Shi LX (2009) Dalton Trans 2009:6790
- López-Alvarado P, Avendaño C, Menéndez JC (1995) J Org Chem 60:5678
- Kang SK, Lee SH, Lee D (2000) Synlett 2000:1022
- Fedorov AY, Finet JP (1999) Tetrahedron Lett 40:2747
- Farahat AA, Boykin DW (2014) Tetrahedron Lett 55:3049

21. Kantam ML, Yadav J, Laha S, Sreedhar B, Jha S (2007) *Adv Synth Catal* 349:1938
22. Yang Q, Wang Y, Yang L, Zhang M (2013) *Tetrahedron* 69:6230
23. Xu ZL, Li HX, Ren ZG, Du WY, Xu WC, Lang JP (2011) *Tetrahedron* 67:5282
24. Liu YS, Liu Y, Ma XW, Liu P, Xie JW, Dai B (2014) *Chin Chem Lett* 25:775
25. Polshettiwar V, Luque R, Fihri A, Zhu H, Bouhrara M, Basset JM (2011) *Chem Rev* 111:3036
26. Astruc D, Lu F, Aranzaes JR (2005) *Angew Chem Int Ed* 44:7852
27. Rout L, Jammi S, Punniyamurthy T (2007) *Org Lett* 9:3397
28. Safaei-Ghomi J, Zahedi S, Ghasemzadeh MA (2014) *Monatsh Chem* 145:1191
29. Mohaqeq M, Safaei-Ghomi J (2015) *Monatsh Chem* 146:1581
30. Alonso F, Riente P, Sirvent JA, Yus M (2010) *Appl Catal A Gen* 378:42
31. Rostamizadeh S, Abdollahi F, Shadjou N, Amani AM (2013) *Monatsh Chem* 144:1191
32. Gupta AK, Gupta M (2005) *Biomaterials* 26:3995
33. Harrison RJ, Dunin-Borkowski RE, Putnis A (2002) *Proc Natl Acad Sci USA* 99:16556
34. Wu W, He Q, Jiang C (2008) *Nanoscale Res Lett* 3:397
35. Esmailpour M, Sardarian AR (2014) *Green Chem Lett Rev* 7:301
36. Esmailpour M, Javidi J, Nowroozi-Dodeji F, Hassannezhad H (2014) *J Iran Chem Soc* 11:1703
37. Esmailpour M, Javidi J (2015) *J Chin Chem Soc* 62:614
38. Esmailpour M, Javidi J (2015) *J Chin Chem Soc* 62:328
39. Esmailpour M, Javidi J, Zahmatkesh S (2016) *Appl Organomet Chem* 30:897
40. Panda N, Jena AK, Mohapatra S, Rout SR (2011) *Tetrahedron Lett* 52:1924
41. Nador F, Volpe MA, Alonso F, Radivoy G (2014) *Tetrahedron* 70:6082
42. Sivakami R, Babu SG, Dhanuskodi S, Karvembu R (2015) *RSC Adv* 5:8571
43. Liu Y, Zhang Q, Ma X, Liu P, Xie J, Dai B, Liu Z (2013) *Int J Org Chem* 3:185
44. Dehghani F, Sardarian AR, Esmailpour M (2013) *J Organomet Chem* 743:87
45. Cristau HJ, Cellier PP, Spindler JF, Taillefer M (2004) *Chem Eur J* 10:5607
46. Emel'yanenko VN, Kaliner M, Strassner T, Verevkin SP (2017) *Fluid Phase Equilib* 433:40
47. Lv X, Wang Z, Bao W (2006) *Tetrahedron* 62:4756
48. Altman RA, Buchwald SL (2006) *Org Lett* 8:2779
49. Yang K, Qiu Y, Li Z, Wang Z, Jiang S (2011) *J Org Chem* 76:3151
50. Inamoto K, Nozawa K, Kadokawa J, Kondo Y (2012) *Tetrahedron* 68:7794
51. Zhang H, Cai Q, Ma D (2005) *J Org Chem* 70:5164
52. Xue F, Cai C, Sun H, Shen Q, Rui J (2008) *Tetrahedron Lett* 49:4386
53. Joseph PJA, Priyadarshini S, Kantam ML, Maheswaran H (2011) *Catal Sci Technol* 1:234
54. Hosseini-Sarvari M, Moeini F (2014) *RSC Adv* 4:7321
55. Esmailpour M, Sardarian AR, Jarrahpour A, Ebrahimi E, Javidi J (2016) *RSC Adv* 6:43376
56. Deng Y, Qi D, Deng C, Zhang X, Zhao D (2008) *J Am Chem Soc* 130:28